Application of linear and nonlinear fracture mechanics criteria for crack propagation analysis in single crystal bodies

Sergey G. Semenov Artem S. Semenov Leonid B. Getsov Boris E. Melnikov
semenov.serg@ksm.spbstu.ru

Abstract

The actual problem of the crack growth prediction in anisotropic elastic and inelastic materials has not been fully investigated neither theoretically nor experimentally. In particular the analysis of crack growth in single-crystal gas-turbine blades is of great interest to assess their strength and durability. The present research is devoted to the comparison of various linear and nonlinear fracture mechanics criteria of the crack propagation in anisotropic materials under different loading conditions (fatigue, thermal fatigue and creep) with published experimental data.

The computational features of the stress intensity factors (SIF) K_I, K_{II}, K_{III}, resolved shear SIF K_{rss}, J-integral and C^*-integral for anisotropic materials in the framework of the finite-element analysis is considered. Verification of implemented procedures for fracture mechanics parameters is carried out on tension specimens of different crystallographic orientations. The results of the edge crack in the single crystal blade of gas-turbine engine simulations are presented and discussed.

1 Introduction

Single crystal nickel-based superalloys are commonly used in parts of gas turbine engines (for example 1st stage high-pressure turbine blades) that are subject to high temperatures and require high strength, excellent high temperature creep and fatigue resistance. The main difficulty during modeling of deformation process of such single crystal materials is a strong anisotropy of elastic and viscoplastic properties [1]. In addition, the prediction of the fracture of single crystal materials has been not fully investigated neither theoretically nor experimentally. There are examples of experimentally approved static strength criteria [2] and crack initiation criteria [3]. However an investigation of the crack propagation process in the monocrystalline bodies with extensive plastic zones under the complex loading is only beginning.

2 Stress intensity factor for anisotropic bodies

Below we use the formalism proposed by Lechnitskii [4]. Direct calculations [5] or calculations with use of the M-integral [6] are used for the stress intensity factor (SIF) evaluation for anisotropic bodies. The complexity of direct SIF computations in the anisotropic case is caused by a mutual coupling of mode I (opening, tensile) and mode II (sliding, in-plane

shear) of a crack [7]:

$$\left\{ \begin{array}{c} K_I \\ K_{II} \\ K_{III} \end{array} \right\} = [B]^{-1} \left\{ \begin{array}{c} u \\ v \\ w \end{array} \right\} \sqrt{\frac{\pi}{2r}}, \tag{1}$$

where u, v, w are components of displacement vector along crack faces perpendicular to front, along perpendicular to crack faces and along crack front correspondingly, r is the distance from the crack front. The matrix $[B]^{-1}$ is introduced by the expression [7]:

$$[B]^{-1} = \left[\begin{array}{ccc} \mathrm{Re}\left[\frac{i}{\mu_1-\mu_2}(q_2-q_1)\right]\frac{1}{D} & \mathrm{Re}\left[\frac{-i}{\mu_1-\mu_2}(p_2-p_1)\right]\frac{1}{D} & 0 \\ \mathrm{Re}\left[\frac{-i}{\mu_1-\mu_2}(\mu_1 q_2-\mu_2 q_1)\right]\frac{1}{D} & \mathrm{Re}\left[\frac{i}{\mu_1-\mu_2}(\mu_1 p_2-\mu_2 p_1)\right]\frac{1}{D} & 0 \\ 0 & 0 & \sqrt{c_{44}c_{55}-c_{45}^2} \end{array} \right], \tag{2}$$

$$D = \left| \begin{array}{cc} \mathrm{Re}\left[\frac{i}{\mu_1-\mu_2}(\mu_1 p_2-\mu_2 p_1)\right] & \mathrm{Re}\left[\frac{i}{\mu_1-\mu_2}(p_2-p_1)\right] \\ \mathrm{Re}\left[\frac{i}{\mu_1-\mu_2}(\mu_1 q_2-\mu_2 q_1)\right] & \mathrm{Re}\left[\frac{i}{\mu_1-\mu_2}(q_2-q_1)\right] \end{array} \right|, \tag{3}$$

where μ_1, μ_2 are complex roots with the positive real part of the characteristic equation

$$a_{11}\mu^4 - 2a_{16}\mu^3 + (2a_{12}+a_{66})\mu^2 - 2a_{26}\mu + a_{22} = 0, \tag{4}$$

where a_{ij}, c_{ij} are elements of the compliance and stiffness matrixes correspondingly, p_k and q_k are defined by expressions:

$$\begin{array}{l} p_k = a_{11}\mu_k^2 + a_{12} - a_{16}\mu_k, \\ q_k = a_{12}\mu_k + \frac{a_{22}}{\mu_k} - a_{26}. \end{array} \tag{5}$$

However, several authors [9, 10, 11] point out that SIFs K_I, K_{II}, K_{III} and their traditional combinations do not adequately describe the fracture process in single crystals. Therefore the resolved shear SIF K_{rss}, taking into account the crystal slip system, was proposed in [9]:

$$K_{rss} = \lim_{r\to 0} \tau_{rss}\sqrt{2\pi r}, \tag{6}$$

where τ_{rss} is the maximum shear stresses in the crystal slip system:

$$\tau_{rss} = \boldsymbol{n}\cdot\boldsymbol{\sigma}\cdot\boldsymbol{l}, \tag{7}$$

where $\boldsymbol{\sigma}$ is Cauchy stress tensor, $\boldsymbol{n}$ is the normal to the slip plane, $\boldsymbol{l}$ is the slip direction, which can be expressed using Burgers vector $\boldsymbol{b}$ as: $\boldsymbol{l} = \boldsymbol{b}/|\boldsymbol{b}|$.

According to experimental data [11, 12, 13] for face-centered single crystal nickel-based superalloys the crack propagation takes place along {111} planes.

3 Invariant contour integrals

The invariant contour integrals or else path-independent integrals [14, 15], which are obtained as a consequence of the energy balance law, can be used for the solving linear and nonlinear fracture mechanics problems. The J-integral should be used instead of SIF, if

a body with crack has extensive plastic zones. The J-integral is defined for an arbitrarily oriented crack (Fig. 1) in two-dimensional (2D) case in the absence of any body forces as:

$$\boldsymbol{J} = J_1\boldsymbol{e}_1 + J_2\boldsymbol{e}_2 = \int_C (W\boldsymbol{n} + \boldsymbol{n}\cdot\boldsymbol{\sigma}\cdot\boldsymbol{u}\nabla)dl, \tag{8}$$

where $\boldsymbol{e}_1, \boldsymbol{e}_2$ are unit vectors of the coordinate system associated with the crack tip, $\boldsymbol{n}$ is external normal to the integration contour C, $\boldsymbol{u}$ - displacement vector. The rigorously correct form of J-integral components is:

$$J_k = \lim_{\varepsilon\to 0}\int_{C_\varepsilon}\left(Wn_k + n_i\sigma_{ij}\frac{\partial u_j}{\partial x_k}\right)dl. \tag{9}$$

In equations (8) and (9) W is the strain-energy density defined as the stress-work through the mechanical strains (without thermal part):

$$W = \int_0^{\boldsymbol{\varepsilon}} \boldsymbol{\sigma}\cdot\cdot\, d\boldsymbol{\varepsilon} = \int_0^t \boldsymbol{\sigma}\cdot\cdot\,\dot{\boldsymbol{\varepsilon}}dt. \tag{10}$$

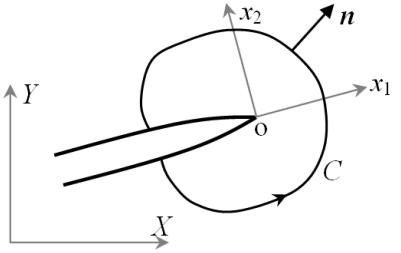

Figure 1: Crack tip and coordinate systems (global (X,Y) and crack system (x_1,x_2)). 2D case.

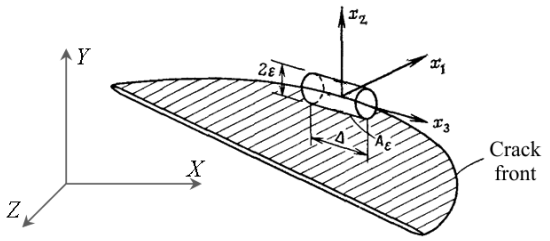

Figure 2: Crack front and coordinate systems (global (X,Y,Z) and crack system (x_1,x_2,x_3)). 3D case.

The generalization of the equation (8) for the 3D case is:

$$\boldsymbol{J} = J_1\boldsymbol{e}_1 + J_2\boldsymbol{e}_2 + J_3\boldsymbol{e}_3 = \frac{1}{\Delta}\int_A (W\boldsymbol{n} + \boldsymbol{n}\cdot\boldsymbol{\sigma}\cdot\boldsymbol{u}\nabla)dA + J_3\boldsymbol{e}_3, \tag{11}$$

where Δ is a length of the tube along crack font (see Fig. 2). Components of the J-integral in 3D case is defined by expressions:

$$\begin{aligned} J_k &= \tfrac{1}{\Delta}\lim_{\varepsilon\to 0}\int_{A_\varepsilon}\left(Wn_k + n_i\sigma_{ij}\tfrac{\partial u_j}{\partial x_k}\right)dA,\ k=1,2 \\ J_3 &= \tfrac{1}{\Delta}\lim_{\varepsilon\to 0}\int_{A_\varepsilon}\left(W_3n_1 + n_i\sigma_{i3}\tfrac{\partial u_3}{\partial x_1}\right)dA, \end{aligned} \tag{12}$$

where W_3 for mode III is:

$$W_3 = \int_0^{\varepsilon_{3j}} \sigma_{3j}\cdot\cdot\, d\varepsilon_{3j} = \int_0^t \sigma_{3j}\cdot\cdot\,\dot{\varepsilon}_{3j}dt. \tag{13}$$

Note, that the components of vectors and tensors in index form correspond to the crack coordinate system (x_1,x_2,x_3).

The invariant contour integral for a viscoelastic material behavior case [16] should be used in the presence of extensive viscous (creep) zones. Such integral can be introduced by analogy with the equation (11):

$$\boldsymbol{C}(t) = C_1(t)\boldsymbol{e}_1 + C_2(t)\boldsymbol{e}_2 + C_3(t)\boldsymbol{e}_3 = \frac{1}{\Delta}\int\limits_A (P\boldsymbol{n} + \boldsymbol{n}\cdot\boldsymbol{\sigma}\cdot\dot{\boldsymbol{u}}\nabla)dA + C_3(t)\boldsymbol{e}_3, \tag{14}$$

$$\begin{aligned} C_k(t) &= \tfrac{1}{\Delta}\lim\limits_{\varepsilon\to 0}\int\limits_{A_\varepsilon}\left(Pn_k + n_i\sigma_{ij}\tfrac{\partial \dot{u}_j}{\partial x_k}\right)dA,\ k=1,2,\\ C_3(t) &= \tfrac{1}{\Delta}\lim\limits_{\varepsilon\to 0}\int\limits_{A_\varepsilon}\left(P_3 n_1 + n_i\sigma_{i3}\tfrac{\partial \dot{u}_3}{\partial x_1}\right)dA, \end{aligned} \tag{15}$$

$$P = \int\limits_0^{\dot{\boldsymbol{\varepsilon}}} \boldsymbol{\sigma}\cdot\cdot\, d\dot{\boldsymbol{\varepsilon}},\ P_3 = \int\limits_0^{\dot{\varepsilon}_{3j}} \sigma_{3j}\cdot\cdot\, d\dot{\varepsilon}_{3j}. \tag{16}$$

During the loading of a viscoelastic material the elastic strain dominates at initial time, but over time the viscous (creep) zone is becoming extensive and the value of $\boldsymbol{C}(t)$ tends asymptotically to the standard fracture mechanics parameter C^* [17].

4 Numerical examples

The relations for the computation of the described above fracture mechanics parameters (1), (6), (11) and (14) for anisotropic materials have been implemented in the finite element program PANTOCRATOR [18]. The parameters SIFs and K_{rss} are calculated numerically using the method based on an extrapolation of displacements and stresses into the crack tip. The path-independent integrals J and C(t) are calculated using the equivalent domain integration (EDI) method [19].

As an illustration the problem of an edge crack in the anisotropic specimen [13] is considered below. The finite element (FE) mesh of the specimen is shown in Fig. 3. The FE model includes 4770 twenty-node isoparametric brick elements with second order of shape functions.

According to the experimental program [13] the FE computations for three different crystallographic orientations (Fig. 3) of the specimens were carried out:

- orientation A: $\langle 00\bar{1}\rangle$ parallel to tensile axis (axis of specimen), $[\bar{1}\bar{1}0]$ perpendicular to the crack front;
- ПЂ orientation B: $\langle 001\rangle$ parallel to tensile axis (axis of specimen), $[0\bar{1}0]$ perpendicular to the crack front;
- orientation C: $\langle \bar{1}11\rangle$ parallel to tensile axis (axis of specimen), $[\bar{1}\bar{1}0]$ perpendicular to the crack front.

In FE computations the loading is applied as uniform pressure on upper and lower specimen faces. The value of pressure corresponds to $K_I = 4MPa\sqrt{m}$ for the equivalent isotropic specimen. The specimens are made from the single crystal alloy UDIMET 720 [13].

The typical von Mises stress field distribution in the specimen is presented in Fig. 4 for loading case A. Calculated SIFs along crack front are shown in Fig. 5. The crystallographic orientation of specimens has significant influence on values of SIFs. Comparison

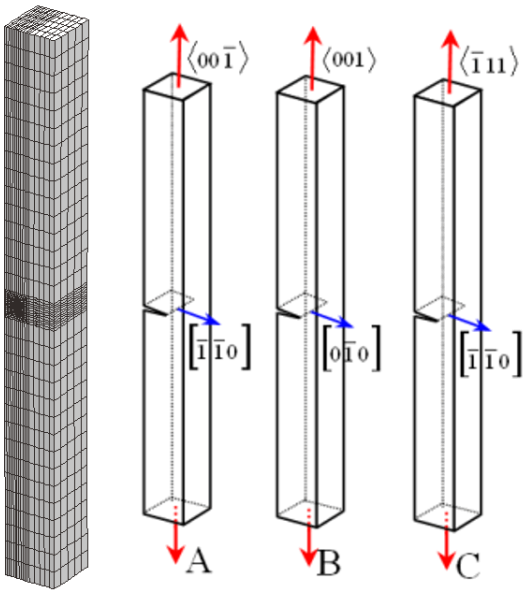

Figure 3: FE model and orientations of the cracked specimens.

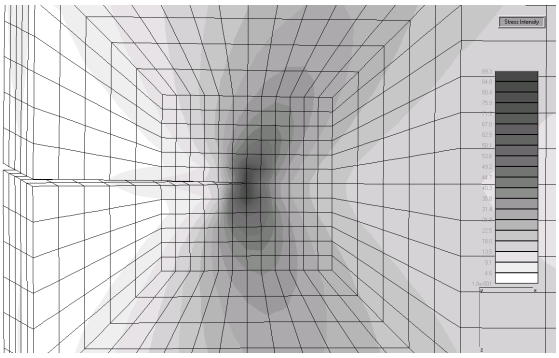

Figure 4: Von Mises stress field in the crack tip neighborhood.

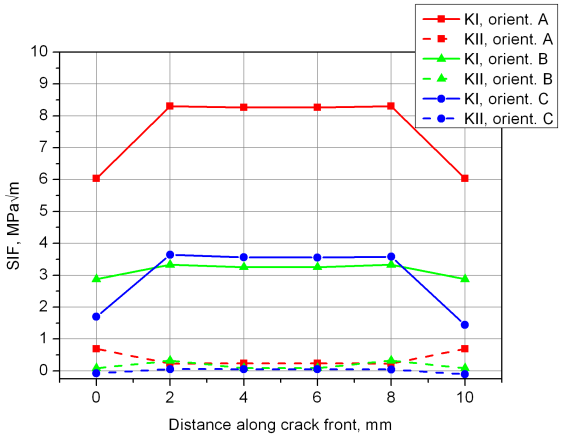

Figure 5: SIFs along crack front.

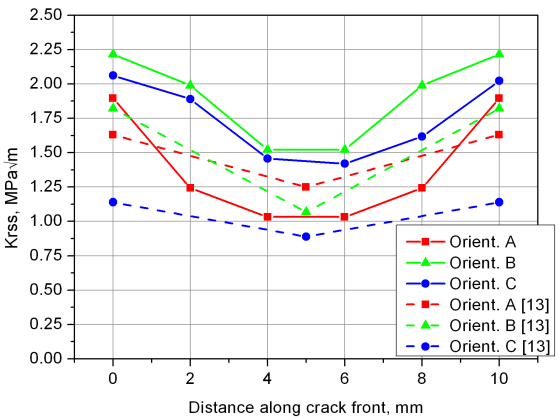

Figure 6: K_{rss} along crack front.

of calculated and experimental [13] distributions of the K_{rss} along crack front shows satisfactory agreement (Fig. 6). The computed values of J-integrals demonstrate invariance to the radius of integration contour

In another example the tensile creep of the viscoelastic plate with an edge crack is considered. The Norton creep model is used. Comparison of simulation results with the simplified analytical approximation $C(t) = C^*(t_T/t + 1)$ is shown in Fig. 7. There is a good agreement for the times corresponding to the extended creep area.

The last example is concerned with the single crystal gas-turbine blade with an edge crack (Fig. 8). The two crack face orientations (001) and (111) are considered and compared for the blade orientation [001]. Distributions of J_1-integral and C_1-integral along crack front are shown in Fig. 9 and 10 for the crack face orientation (001). The distributions indicate that the progressive growth of fatigue and creep cracks takes place in the middle of the crack front.

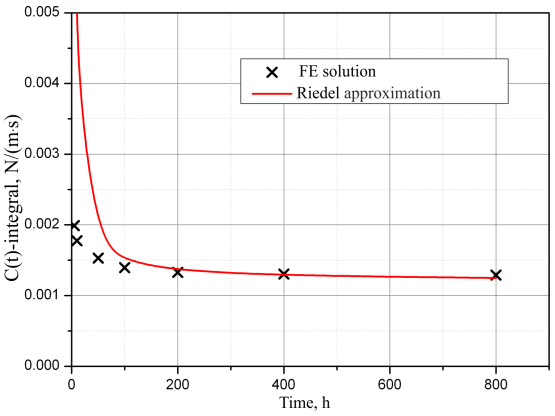

Figure 7: C(t)-integral evolution for the plate with an edge crack.

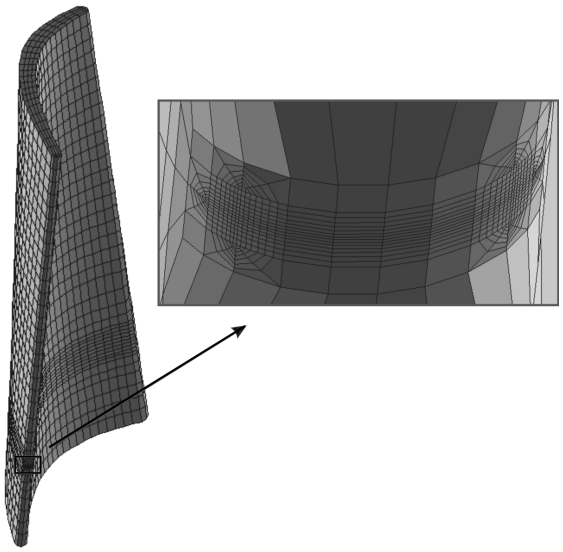

Figure 8: FE model of the single crystal turbine blade with an edge crack.

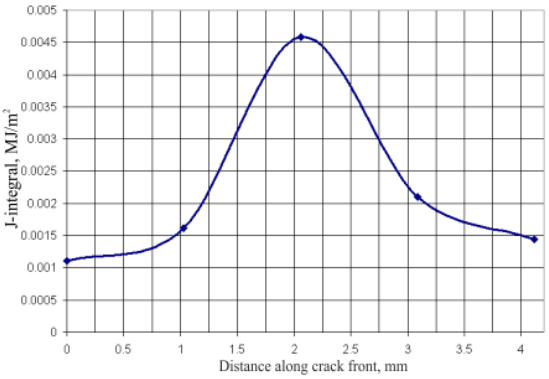

Figure 9: J_1-integral along crack front.

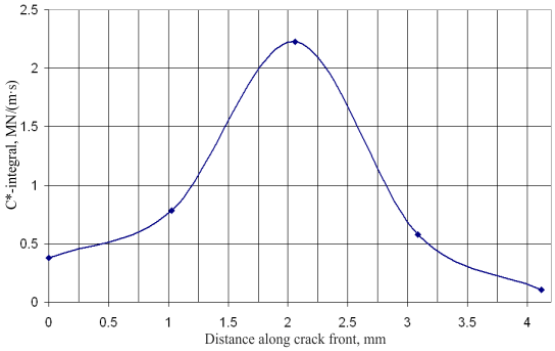

Figure 10: C_1^*-integral along crack front.

Conclusions

A wide range of linear and nonlinear fracture mechanics methods for anisotropic materials has been considered, implemented in the FE program PANTOCRATOR and compared in simulations. Verification of implemented procedures is carried out on tension specimens of different crystallographic orientations. The further experimental studies are required for the description of fatigue, thermal fatigue and creep cracks propagation in single crystals.

Acknowledgements

The study was partially supported by the RFBR research project 12-08-00-943a and by British Petroleum research grant.

References

[1] Besson J., Cailletaud G., Chaboche J.-L., Forest S. Non-linear mechanics of materials. Springer, 2010.

[2] Getsov L.B., Semenov A.S., Tikhomirova E.A, Rybnikov A.I. Failure criteria for single crystal alloys of gas turbine blades under static and thermocyclic loading. Proc. 19th European Conference on Fracture. Fracture Mechanics for Durability, Reliability and Safety. 2012. P. 670-678.

[3] Semenov A.S., Semenov S.G., Nazarenko A.A., Getsov L.B. Computer simulation of fatigue, creep and thermal-fatigue cracks propagation in gas-turbine blades. Materials and Technology. 2012; 46(3): 197-203.

[4] Lekhnitskii S.G. Theory of Elasticity of an Anisotropic Body. San Francisco: Holden-Day, 1950, in Russian, 1963, in English, translated by Fern P.

[5] Ranjan S., Arakere N.K. A Fracture-Mechanics-Based Methodology for Fatigue Life Prediction of Single Crystal Nickel-Based Superalloys. J. Eng. Gas Turbines Power 130, 032501, 2008.

[6] Yau J.F., Wang S.S., Corten H.T. A mixed-mode crack analysis of isotropic solids using conservation laws of elasticity. J Appl. Mech. 1980; 47: 335-341.

[7] Ranjan S. Development of a Numerical Procedure for Mixed Mode K-Solutions and Fatigue Crack Growth in FCC Single Crystal Superalloys. Ph.D. thesis, University of Florida. 2005.

[8] Chen Q., Liu H.W. Resolved shear stress intensity coefficient and fatigue crack growth in large crystals, NASA, Syracuse University, Contractor Report No. CR-182137. 1988.

[9] Telesman J, Ghosn L.J. The unusual near-threshold FCG behaviour of a single crystal superalloy and the resolved shear stress as the crack driving force. Engng. Fract. Mech. 1989; 34(5/6): 1183вЂ“1196.

[10] Antolovich B.F., Saxena A., Antolovich S.D. Fatigue Crack Propagation in Single-Crystal CMSX-2 at Elevated Temperature. Journal of Materials Engineering and Performance. 1993.

[11] Chan K.S., Hack J.E., Liverant G.R. Fatigue crack growth in MAR-M200 single crystals. Met. Trans. 1987; 18(4): 581-591.

[12] Chan K.S., Cruse T.A. Stress intensity factors for anisotropic compact-tension specimens with inclined cracks. Engng. Fract. Mech. 1986; 23(5): 863-874.

[13] Reed P.A.S., Wu X.D., Sinclair I. Fatigue crack path prediction in UDIMET 720 nickel-based alloy single crystals. Metall Mater Trans. A 2000; 31A: 109–123.

[14] Rice J.R. A path-independent integral and the approximate analysis of strain concentration by notches and cracks. J. appl. Mech. 1968; 35: 376-386.

[15] Cherepanov G.P. Crack propagation in continuous media. J. Appl. Math. Mech. 1967; 31: 503-512.

[16] Landes J.D., Begley J.A. A fracture mechanics approach to creep crack growth. In: Mechanics of Crack Growth, ASTM STP 590. Am. Soc. Testing Mat. 1976. P. 128-148.

[17] ASTM E1457-07e4 Standard Test Method for Measurement of Creep Crack Growth Times in Metals.

[18] Semenov A.S. PANTOCRATOR – the finite element program specialized on the non-linear problem solution. Proceedings of the Vth international conference on scientific and engineering problems of predicting the reliability and service life of structures. St.-Petersburg. 2003. P. 466-480.

[19] Nikishkov G.P., Atluri S.N. An equivalent domain integral method for computing crack-tip integral parameters in non-elastic, thermomechanical fracture. Engng Fracture Mech. 1987; 26: 851-867.

Sergey G. Semenov, Politechnicheskaya str. 29, Saint-Petersburg, Russia
Artem S. Semenov, Politechnicheskaya str. 29, Saint-Petersburg, Russia
Leonid B. Getsov, Politechnicheskaya str. 29, Saint-Petersburg, Russia
Boris E. Melnikov, Politechnicheskaya str. 29, Saint-Petersburg, Russia